

# Deuteron-induced reaction cross sections for $^{93}\text{Zr}$ up to 200 MeV

Marilena Avrigeanu<sup>1,\*</sup> and Vlad Avrigeanu<sup>1</sup>

<sup>1</sup>Horia Hulubei National Institute for Physics and Nuclear Engineering, P.O. Box MG-6, 077125 Bucharest-Magurele, Romania

**Abstract.** The analysis of the deuteron-induced reactions on  $^{93}\text{Zr}$  target nucleus is carried out paying due consideration to the nuclear reaction mechanisms associated to the deuteron interaction process. The role of breakup reaction mechanism is underlined by the comparison of data with theoretical and evaluation predictions.

## 1 Introduction

The increased interest in deuteron interaction process is the result of high accuracy deuteron nuclear data request coming from the large international projects ITER, Fusion Materials Irradiation Facility (IFMIF), SPIRAL2 and SARAF accelerators [1], as well as from medical investigations using deuterons beam, and most recently from nuclear-waste treatment analysis devoted to the transmutation of long-lived residual nuclei into short-lived or even stable nuclei [2]. The selection of the structural materials involved in these projects requires the analysis of the deuteron-induced damage and degradation properties as well as of the various level of radioactivity through initiated nuclear reactions. Therefore, complementary research programmes devoted to the update of both the experimental nuclear data systematics and the theoretical frame of the data analysis have been started as FENDL library and the EUROfusion programme [3].

While recent advancements in deuteron reaction modeling in the TALYS code [4] are taken into account to provide more reliable data, current discrepancies between experimental and calculated data follow the incomplete theoretical frame of deuteron interactions requesting, besides the pre-equilibrium emission (PE) and fully equilibrated compound nucleus (CN) decay, consistent inclusion of the breakup mechanism (BU) and direct reactions (DR) contributions [5, 6]. Actually, the due consideration of the deuteron BU has to take into account two opposite effects, namely the important BU leakage of initial flux as well as the BF enhancement brought by the BU-nucleon interactions with the target nucleus (e.g., [6, 7]). Thus, an extended analysis of the deuteron interaction with the target nuclei common in the alloys of candidate materials for ITER and IFMIF installations already concerned the stable isotopes of Al, Cr, Mn, Fe, Co, Ni, Zr, Nb, and Mo for deuteron energies until 50 MeV ([8, 9] and Refs. therein).

An opportunity to extend the incident energy range of the above-mentioned approach was provided by Chillery-Nakano-Kawase [2, 10, 11] studies devoted to the resid-

ual nuclei population by  $^{93}\text{Zr}$  radioactive beam interaction with a deuteron gas target. The long-lived fission product  $^{93}\text{Zr}$  radioactive nucleus ( $T_{1/2} = 1.61$  M yr) rises questions concerning the waste treatment, strongly related to the investigation of various reactions leading to short-lived or even stable residual nuclei. The recent comparison of Chillery et al. [2] calculations performed using DEURACS [12] and TALYS-1.96 [4] codes for  $^{93}\text{Zr}(d,x)$  activation cross sections has represented a challenge for checking the predictions of our previous results of the  $^{nat}\text{Zr}(d,x)$  activation analysis [9] within the above-mentioned framework.

## 2 Nuclear reaction mechanisms

**Breakup.** The theoretical frame involved also for the deuteron interaction analysis with  $^{93}\text{Zr}$  target nucleus includes the consideration of the deuteron BU as well as DR, PE, and CN reaction mechanisms. Details regarding the physical picture of the deuteron breakup in the Coulomb and nuclear fields of the target nucleus were given recently [6, 9]. Accordingly, only particular points are mentioned hereafter for the distinct processes that are considered in this respect, namely the elastic breakup (EB) in which the target nucleus remains in its ground state without no interaction with the deuteron constituents, and the inelastic breakup [13] or breakup fusion (BF) [14] where a breakup nucleon interacts non-elastically with the target nucleus (named more recently non-elastic breakup, NEB [2, 12]).

Empirical parametrization [7], has concerned the ratios of elastic and total breakup proton-emission to the deuteron reaction cross section  $\sigma_R$ , i.e.  $\sigma_{EB}/\sigma_R$  and  $\sigma_{BU}^p/\sigma_R$ , respectively. Under the assumption of equal neutron- and proton-breakup cross sections [14], the BF fraction is given by the difference  $f_{BF}^{n/p} = f_{BU}^{n/p} - f_{EB}$  as well.

The comparison of the experimental proton breakup  $f_{BU}^p$  and elastic breakup  $f_{EB}$  fractions [13, 14], and parametrization results is shown in Fig. 1 for deuterons incident on target nuclei from  $^{27}\text{Al}$  to  $^{232}\text{Th}$ , including  $^{90}\text{Zr}$ , [Fig. 1(g)], at energies up to 80 MeV – the incident energy upper limit of the breakup cross-section measurements.

\*e-mail: marilena.avrigeanu@nipne.ro

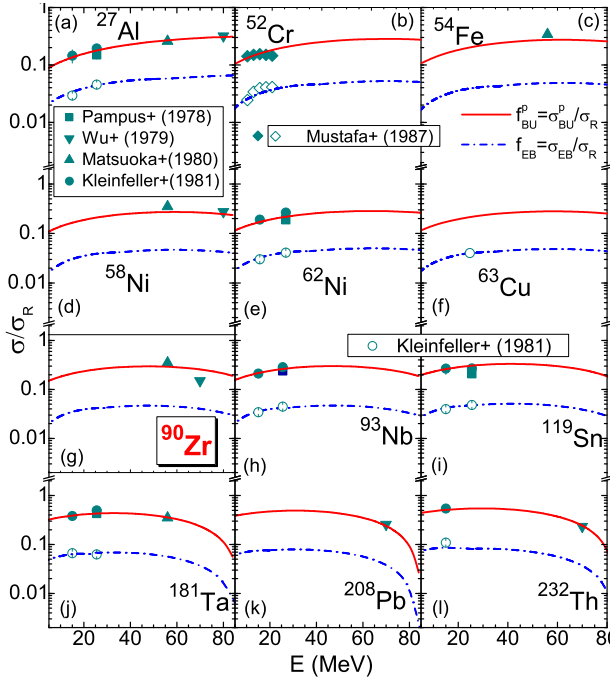


**Figure 1.** Comparison of experimental [13, 15] total breakup proton-emission (solid symbols) and elastic-breakup (open circles) fractions, and the corresponding parametrizations [7] (solid and dash-dotted curves, respectively) for deuterons incident on nuclei from  $^{27}\text{Al}$  (a) to  $^{232}\text{Th}$  (l) at energies up to 80 MeV,

Concerning the BU mechanism analysis for deuterons interaction with  $^{93}\text{Zr}$  target nucleus the total BU, total BU *nucleon*-emission, inelastic-breakup *nucleon* emission, and EB excitation functions are shown together with those corresponding to the adjacent isotopes  $^{92,94}\text{Zr}$  [9] in the upper part of Fig. 2. The analysis of breakup mechanism for  $^{93}\text{Zr}$  isotope was extended to 110 MeV where, following the decreasing behavior with incident energy increase over  $\sim 60$  MeV shown in Fig. 1, the phenomenological breakup cross sections vanish. This variation of breakup cross section with deuteron energy explains the diminution of the inelastic breakup enhancement, until an apparent disappearance in Fig. 3 around  $E=100$  MeV.

Nevertheless, the BF component is dominant among BU components shown in Fig. 2. This feature is quite important for the analysis of two opposite BU effects on deuteron-activation cross sections, briefly recalled hereinafter. First, the total-reaction cross section, that is shared among different outgoing channels, is reduced by the value of  $\sigma_{BU}$ . Second, on the other hand, the BF component brings additional contributions to different reaction channels of the deuteron-nucleus interaction [6, 8, 9]. Thus, interactions of the breakup protons or neutrons with the target nucleus contribute to enhancement of the corresponding  $(d, xn)$  or  $(d, xp)$  reaction cross sections, respectively. The compound nuclei in reactions induced by the breakup nucleons differ by one unit of  $A$  and maybe of also  $Z$  from those in deuteron-induced reactions. The partition of the BF cross section among various residual-nuclei population is triggered by the energy spectra of the breakup nucleons

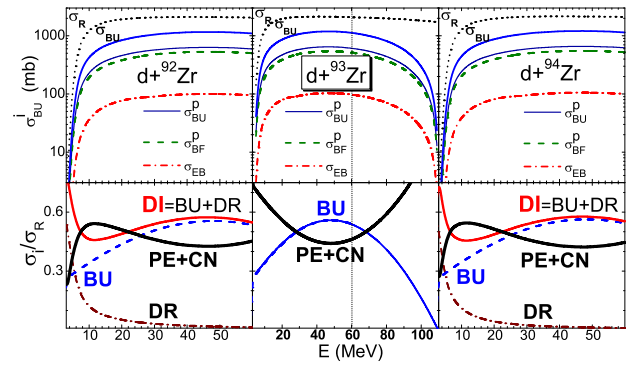


**Figure 2.** (Upper) Excitation functions corresponding to deuteron total reaction  $\sigma_R$  (thick dotted curves), total BU  $\sigma_{BU}$  (thick curves), *nucleon* total BU  $\sigma_{BU}^p$  (thin solid), *nucleon* inelastic-breakup  $\sigma_{BF}^p$  (dashed), and elastic-breakup  $\sigma_{EB}^p$  (dash-dotted) [7] of deuteron interactions with  $^{92,93,94}\text{Zr}$  isotopes. (Lower)  $\sigma_R$  fractions of BU (thin solid), DR (dashed), DI (thick solid), and PE+CN (dotted curves) cross sections of deuteron interactions with  $^{92,93,84}\text{Zr}$  target nuclei (see text).

and the excitation functions of the reactions induced by these nucleons on the target nuclei [6, 7].

In order to calculate the BF enhancement of, e.g., the  $(d, xn)$  reaction cross sections, the BF proton-emission cross section  $\sigma_{BF}^p$  should be (i) multiplied by the proton-enhancing ratios  $\sigma_{(p,x)}/\sigma_R^p$ , (ii) convoluted with the Gaussian line shape distribution of the BF-proton energy  $E_p$  for a given deuteron incident energy  $E$ , and (iii) integrated over the BF-proton energy. Consequently, the BF-enhancement cross section has the form [6]:

$$\sigma_{BF}^{p,x}(E) = \sigma_{BF}^p(E) \int dE_p \frac{\sigma_{(p,x)}(E_p)}{\sigma_R^p} \frac{1}{(2\pi)^{\frac{1}{2}} w} \exp\left[-\frac{(E_p - E_p^0(E))^2}{2w^2}\right], \quad (1)$$

where  $\sigma_R^p$  is the proton total-reaction cross section,  $x$  stands for various  $\gamma$ ,  $n$ ,  $d$ , or  $\alpha$  outgoing channels, while Kalbach Gaussian parameters  $w$  and  $E_p^0$  [16] were used.

The enhancements due to  $(p, x)$  and  $(n, x)$  reactions induced by the breakup nucleons on  $^{93}\text{Zr}$  are shown by dotted curves in Fig. 3 (Sec. 3). It has been thus proved that BF enhancements are particularly important for the suitable description of the maximum as well as the high-energy side of the excitation functions for second and third chance emitted-particle channels [6, 9]. The above-mentioned BU cross-section parametrization as well as the inelastic-breakup enhancement are included in TALYS-1.96 code [4], for *breakupmodel* keyword 2.

**Direct reactions.** Apart from the BU contributions to deuteron interaction, the *stripping*,  $(d, p)$  and  $(d, n)$ , and *pick-up*,  $(d, t)$  and  $(d, \alpha)$  direct reactions [8], are quite important for the population of the residual nuclei corresponding to first-chance particle emission channels. However, the estimation of DR cross sections is conditioned by the available experimental spectroscopic factors, outgoing particle angular distributions, or at least the differential cross-section maximum values. The lack of any spectro-

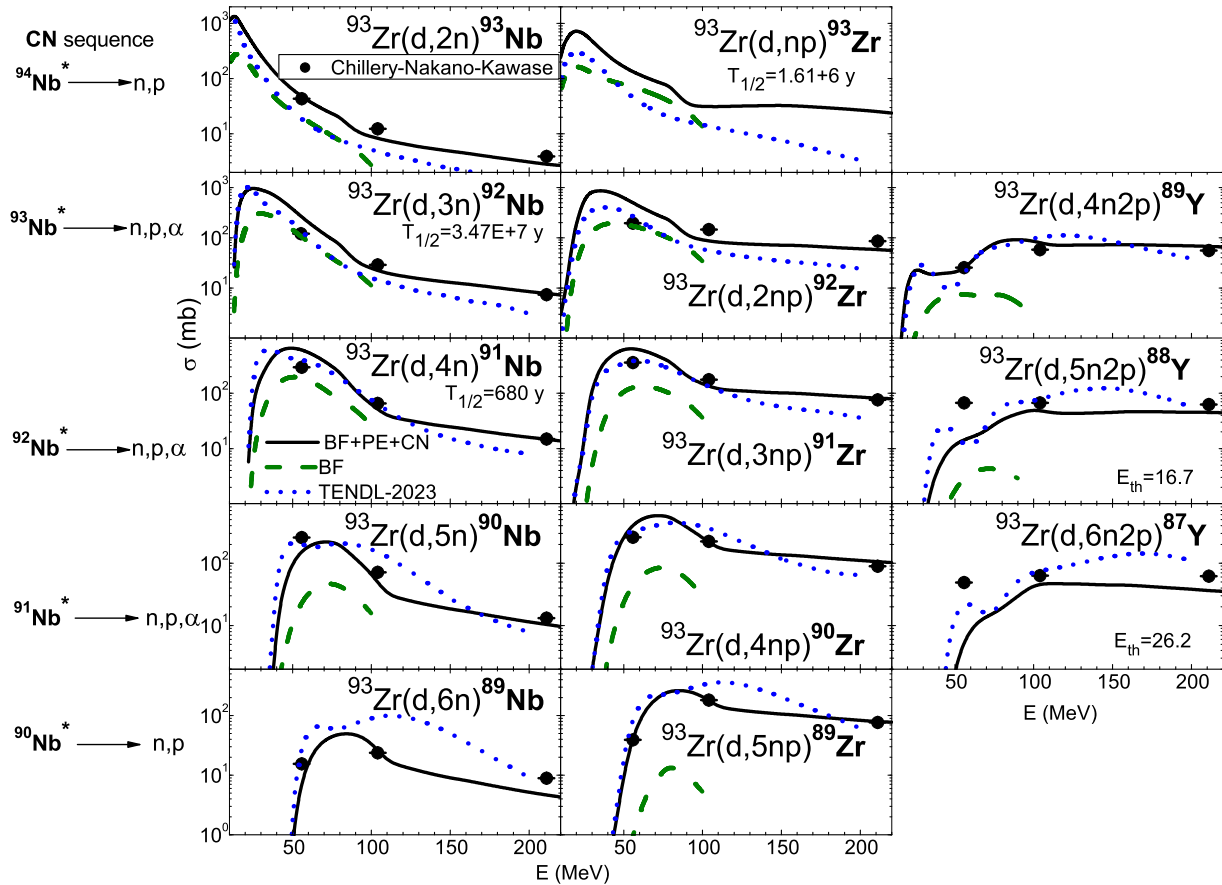


**Figure 3.** Comparative analysis of measured excitation functions of residual nuclei populated by  $d+^{93}\text{Zr}$  interaction [2, 10, 11] along with TENDL–2023 evaluation predictions [18] (dotted curves), and model calculations (solid) including BF enhancements (dashed).

scopic informations concerning both stripping and pick-up processes initiated by deuterons on  $^{93}\text{Zr}$  is the reason of missing of the corresponding DR contribution to population of various residual nuclei, within present analysis.

**Statistical particle emission.** The statistical PE+CN reaction mechanisms become important with the increase of the incident energy above the Coulomb barrier. The corresponding  $d+^{93}\text{Zr}$  activation cross sections have been calculated in this work using TALYS-1.96 code [4] and taking into account also the above-discussed BU through *breakupmodel 2* option. However, the direct reaction (DR) mechanism contribution has been missing due the lack of any specific spectroscopic information. The parameter sets within the analysis of  $d+^{nat}\text{Zr}$  activation process [9], have also been involved for this isotope, i.e., (a) the OMPs of Koning-Delaroche, Daehnick et al., Becchetti-Greenlees, and Avrigeanu et al. for neutrons and protons, deuterons, tritons, and  $\alpha$  particles, respectively [17], (b) the back-shifted Fermi gas (BSFG) formula for the nuclear level density, and the analytical PE transition rates with energy-dependent matrix element [4, 9].

The particular point of our model calculations is the use of the same model parameters sets to account for different reaction mechanisms as, e.g., the same OMP parameters for calculation of the breakup cross sections, the PE

transition rates, as well as the transmission coefficients of various ingoing/outgoing CN channels.

### 3 Results and Discussion

The importance of the reaction mechanisms involved in deuterons interaction with  $^{92,93,94}\text{Zr}$  target nuclei is shown in the lower part of Fig. 2 by  $\sigma_R$  fractions of BU, DR, direct interaction processes  $\text{DI}=\text{BU}+\text{DR}$ , and PE+CN cross sections. The DR contributions have also been taken into account to estimate the total-reaction cross section that remains available for the PE+CN mechanisms due the incident flux leakage through the BU and DR direct interaction processes, for  $^{92,94}\text{Zr}$  isotopes [9]. One may note that the steep increase with energy of PE+CN fraction at low incident energies in the case of these isotopes [9] is replaced, in the case  $^{93}\text{Zr}$ , by a maximum at lowest incident energies. It is obvious that there is no considered contribution of the DR mechanisms for this isotope, while the breakup mechanism is still weak. The BU mechanism contribution also increases with the increase of the incident energy, leading to the decrease of the deuteron reaction cross section that remains available for the PE+CN statistical mechanisms. Then, the decrease of BU mechanism importance for incident energies over 60 MeV, which is the case of  $^{93}\text{Zr}$  target nucleus, leaves room for PE+CN increase.

The measured excitation functions of residual nuclei of deuteron interaction with  $^{93}\text{Zr}$  [2, 10, 11] are compared in Fig. 3 with results of calculations using TALYS [4] code including the breakup enhancement option, and the newest evaluation given by TENDL-2023 [18]. Thus, it can be seen that the strong contribution of the inelastic breakup enhancement to the population of residual nuclei accompany two, three and four particle emission, i.e.  $(d, 2n)$ ,  $(d, np)$ ,  $(d, 3n)$ ,  $(d, 2np)$ ,  $(d, 4n)$ , and  $(d, 3np)$  respectively. The decay sequence of the compound nuclei corresponding to  $d+^{93}\text{Zr}$ , starting with the second one in the decay sequence,  $^{94}\text{Nb}$ , is added at the left side of this figure. The most important chains of decay,  $n$ ,  $p$ ,  $\alpha$  are also shown in the sequence of decay of the compound nucleus corresponding to the measured residual nuclei. The same scale is kept for the decay line of a compound nucleus in order to stress out the importance of the various residual channels. As it was above-mentioned within analysis of the BU cross sections shown in Figs. 1 and 2, the corresponding phenomenological breakup enhancement excitation functions (dotted curves in Fig. 3) vanish around 100 MeV [6].

Overall, the theoretical predictions describe satisfactory the less the apparent underestimation of  $^{87,88}\text{Y}$  population data at 56 MeV. Apart the sequential nucleons emission, the  $\alpha$ -particle evaporation is involved within these  $(d, 4n\alpha)$  and  $(d, 3n\alpha)$  channels, respectively. It results that additional investigation of specific residual nuclei structure, besides the parameter sets involved in our former  $d+^{nat}\text{Zr}$  analysis [9], as well as new measurements could be useful. As already noted [9], continuous interest in the breakup theoretical analysis, e.g. [19], could also provide improved deuteron-breakup empirical parametrization and more accurate activation cross sections.

## 4 Conclusions

Following the theoretical analysis of  $d+^{nat}\text{Zr}$  [9], the present work emphasizes an additional check of the actual deuteron interactions framework and corresponding predictions. It is indeed supported by the comparison of the recent experimental data and the present calculations, as well as the corresponding TENDL-2023 evaluation [18]. Distinct discrepancies can be obviously related to the complexity of the interaction process, not entirely accounted for in routine evaluation/theoretical analyzes. Nevertheless, the upgrade of the theoretical assumptions for the deuteron interaction processes demands also an overall increase of the deuteron data basis. Concerning the appropriateness of the reaction  $d+^{93}\text{Zr}$  for the treatment of radioactive waste, the incident energy should be over 200 MeV to avoid the maximum population of two other long-lived residual nuclei, namely  $^{91,92}\text{Nb}$ , as shown in Fig. 3.

This work has been partly supported by The Executive Unit for the Financing of Higher Education, Research, Development and Innovation (UEFISCDI) (Project No. PN-III-ID-PCE-2021-0642) and carried out within the framework of the EUROfusion Consortium, funded by the European Union via the Euratom Research and Training Programme (Grant Agreement No

101052200 — EUROfusion). Views and opinions expressed are however those of the author(s) only and do not necessarily reflect those of the European Union or the European Commission. Neither the European Union nor the European Commission can be held responsible for them.

## References

- [1] [www.iter.org](http://www.iter.org); [www.ifmif.org](http://www.ifmif.org); [www.ganil-spiral2.eu](http://www.ganil-spiral2.eu); [www.gov.il/en/pages/facilitysaraf](http://www.gov.il/en/pages/facilitysaraf)
- [2] T. Chillery et al., Prog. Theor. Exp. Phys. 121D01 (2023)
- [3] FENDL-3.0: Fusion Evaluated Nuclear Data Library, <https://www-nds.iaea.org/fendl30/>
- [4] A.J. Koning, S. Hilaire, S. Goriely, v. TALYS-1.96, 2022, <https://nds.iaea.org/talys/>; A.J. Koning, S. Hilaire, S. Goriely, Eur. Phys. J. A **59**, 131 (2023)
- [5] U. Fischer et al., Fus. Eng. and Des. **136**, 162 (2018)
- [6] M. Avrigeanu et al., Eur. Phys. J. A **58**, 3 (2022)
- [7] M. Avrigeanu et al., Fusion Eng. Design **84**, 418 (2009); M. Avrigeanu, A.M. Moro, Phys. Rev. C **82**, 037601 (2010); M. Avrigeanu, V. Avrigeanu, Phys. Rev. C **92**, 021601 (2015); *ibid.* **95**, 024607 (2017)
- [8] P. Bém et al., Phys. Rev. C **79**, 044610 (2009); E. Šimečková et al., *ibid.* **84**, 014605 (2011); M. Avrigeanu, V. Avrigeanu, A.J. Koning, *ibid.* **85**, 034603 (2012); M. Avrigeanu et al., *ibid.* **88**, 014612 (2013); *ibid.* **89**, 044613 (2014); *ibid.* **94**, 014606 (2016); E. Šimečková et al., *ibid.* **98**, 014606 (2018); I. Mardor et al., Eur. Phys. J. A **54**, 91 (2018); M. Avrigeanu et al., Phys. Rev. C **101**, 024605 (2020); M. Avrigeanu et al., J. Fusion Energy **43**, 15 (2024)
- [9] M. Avrigeanu et al., Phys. Rev. C **104**, 044615 (2021)
- [10] K. Nakano et al., EPJ Web Conf. **239**, 20006 (2020)
- [11] S. Kawase et al., Prog. Theor. Exp. Phys. 093D03 (2017)
- [12] S. Nakayama et al., Phys. Rev. C **98**, 044606 (2018)
- [13] J. Pampus et al., Nucl. Phys. **A311**, 141 (1978); J. Kleinfeller et al., Nucl. Phys. A **370**, 205 (1981); G. Baur et al., Phys. Rep. **111**, 333 (1984)
- [14] M.G. Mustafa et al., Phys. Rev. C **35**, 2077 (1987)
- [15] J.R. Wu et al., Phys. Rev. C **19**, 370 (1979); N. Matsuoka et al., Nucl. Phys. **A345**, 1 (1980)
- [16] C. Kalbach Walker, <https://www-nds.iaea.org/fendl3/docs/dBreakupRCM2.pdf>
- [17] A.J. Koning, J.P. Delaroche, Nucl. Phys. A **713**, 231 (2003); W.W. Daehnick et al., Phys. Rev. C **21**, 2253 (1980); F. D. Becchetti, Jr. and G. W. Greenlees, John H. Williams Laboratory Annual Report 1969 (Minnesota Univ., Minneapolis, 1969), p. 116 ; V. Avrigeanu et al., Phys. Rev. C **49**, 2136 (1994)
- [18] A.J. Koning et al., Nuclear Data Sheets **155**, 1 (2019); [https://tendl.web.psi.ch/%\\$%{tendl\\_2023/Zr/DeuteronZr93.html}](https://tendl.web.psi.ch/%$%{tendl_2023/Zr/DeuteronZr93.html)
- [19] J. Lei and A.M. Moro, Phys. Rev. C **92**, 044616 (2016); *ibid.* **97**, 011601 (2018); Y.S. Neoh et al., *ibid.* **94**, 044619 (2016); K. Ogata and K. Yoshida, *ibid.* **94**, 051603 (2016); G. Potel et al., Eur. Phys. J. A **53**, 178 (2017)